Supplementary Material

Molecular Dynamics and Brownian Dynamics Investigation of Ion Permeation and Anesthetic Halothane Effects on a Proton−gated Ion Channel

Mary Hongying Cheng[†], Rob D. Coalson [†]* and Pei Tang[‡¶#]*

Department of [†]Chemistry, Departments of [‡]Anesthesiology, [¶]Pharmacology and Chemical Biology, and [#]Computational Biology, University of Pittsburgh, Pittsburgh, PA 15260

I. Putative anesthetic halothane binding sites

Anesthetic halothane binding sites in GLIC were predicted through flexible docking using the Autodock program[1] (version 3.0.05) on the original crystal structure of GLIC (PDB: 3EAM) and snapshots of GLIC extracted after 5-ns MD simulations. 500 independent docking runs were performed using a Lamarckian genetic algorithm (LGA). A grid spacing of 0.375 Å and grid size of 256×256×280 were utilized to span the entire protein structure. The maximum number of energy evaluations was set to 25,000,000. Three important binding sites predicted by this analysis are: A) inter−subunit site near TM23 loop; B) inter−subunit site near D86; and C) intra−subunit site near W160. The docking energy is in the range of -3.4 Kcal/mol to -3.2 Kcal/mol for these sites, which is equivalent to an apparent dissociation constant K_d of 3.5 mM to 4.9 mM. Detailed halothane binding pockets are illustrated in Fig. S1. Sites A and C are compatible with our recent fluorescence quenching experimental study. [2]

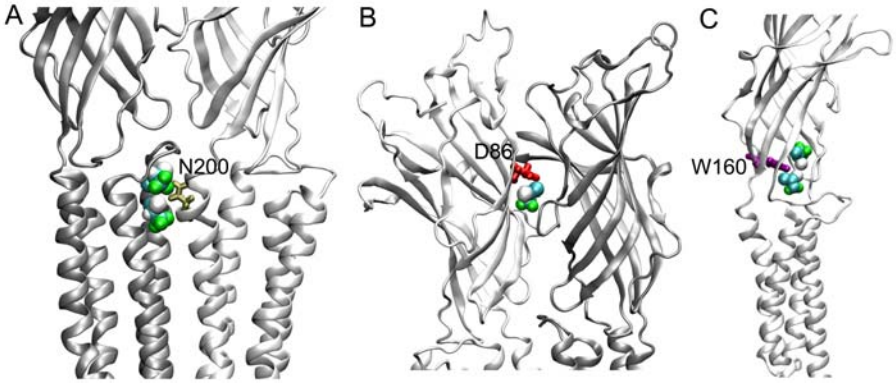

Figure S1: A). Inter−subunit sites near TM23 loop and N200 from the TM1; B) Inter−subunit site near D86; and C). Intra−subunit site near W160. Halothane molecules are shown in VDW format and protein residues are presented in licorice format. Different protein subunits are colored in white and gray.

II. Preparation of MD simulation systems

The simulation systems were setup using the VMD package.[3] The protonation state of titratable residues of GLIC at pH = 4.6 was estimated based on the pKa calculations by Bocquet et al.[4] The distribution of protonated residues among five subunits was determined based on a calculation using the Henderson−Hasselbalch equation.[5,6] Generally, three or four among five subunits of acidic residues (including E26, E35, E67, E69, E75, E82, D86, D88, E177, and E243) were randomly chosen to be protonated (neutralized). H127 was protonated (assigning

+1e). H235 and H277 were deprotonated since they were embedded in the protein. A binary POPE−POPG lipid mixture [7] in a ratio of 3:1 was prepared and equilibrated for 2ns to mimic the bacterial cell membrane. The TM domain of the GLIC was embedded in this equilibrated lipid patch and the remaining part of GLIC was fully solvated by TIP3P water (cf. Fig.1). To fine tune the protonation states of E222 residues, three different systems were constructed: in System A, two E222 residues were protonated; in System B, three E222 residues were protonated; and in System C, none of E222 residues were protonated. In all systems, Na^+ and Cl^- ions were added appropriately in order to neutralize the system. System A contained 1GLIC, 263 POPE, 80 POPG, 80 Na^+, 11 Cl^- and 33,277 water molecules for a total of 168,430 atoms. The GLIC in System A carried an overall positive charge of +11 e.

In the present study, two MD simulation halothane systems were constructed: 1) 10 halothane molecules docked in the crystal structure (termed as 10HAL); and 2) two halothane molecules docked near W160 (termed as HAL−Near−W160) in a structure subjected first to 5ns MD simulation, which produced a stably bound halothane-protein system. Fig. S2 shows the setup of the two halothane systems used in MD simulations. These halothane systems were identical to System A except for the additional halothane molecules at the sites indicated above (and in Fig. S2).

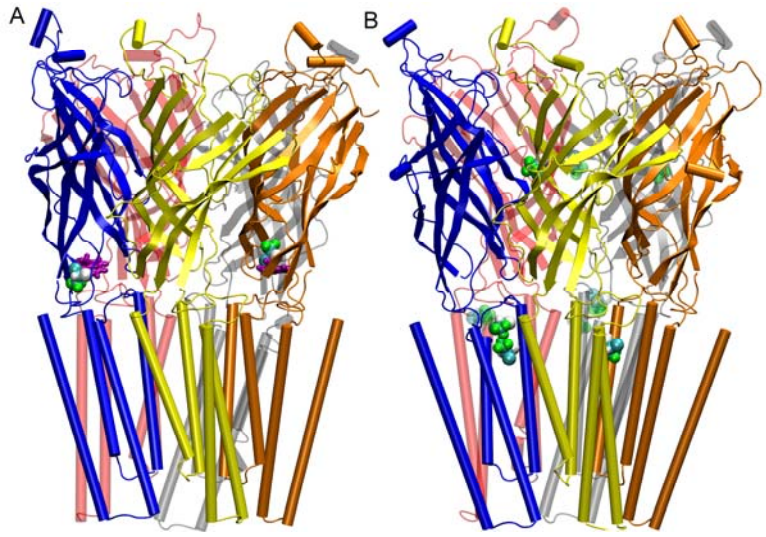

Figure S2: Halothane systems for MD simulations. For clarity, only halothane molecules and GLIC are shown. (A) HAL−Near−W160 system, in which two halothane molecules were docked to the sites near W160 (purple licorice format). (B) 10HAL system, in which seven halothanes were docked to sites near TM23 loops and three were docked near D86 in the EC domains. Halothane binding sites near W160 and TM23 loops are consistent with our recent fluorescence quenching experiments. [2]

III. MD simulation protocols.

MD simulations were performed using the NAMD package[8] with the CHARMM27 force field (version 31).[9] Production runs were carried out without any restraint and under Nosé−Hoover constant pressure (P = 1 Bar) and temperature (T = 310 K) (NPT).[10,11] Periodic boundary conditions and water wrapping were applied. Hydrogen atoms were constrained via SHAKE, and long range electrostatic forces were evaluated via the Particle Mesh Ewald (PME) algorithm.[12] The bonded interactions and the short−range non−bonded interactions were calculated at every time step (1 fs) and every two time steps, respectively. Electrostatic interactions were calculated every four time steps. The cutoff distance for non−bonded

interactions was 10 Å. A smoothing function was employed for the van der Waals interactions at a distance of 8.5 Å. The pair list of the non−bonded interaction was calculated every 20 time steps with a pair list distance of 11.5Å.

IV. MD calculations of single ion potential of mean force (PMF)

The single ion PMFs for transporting a Na^+ or Cl^- ion through the protein channel of our simulation systems were calculated using the adaptive biased force (ABF) method[13,14] implemented in NAMD and following a previous calculation for Cys−loop receptors.[15] All simulation systems were equilibrated for 5 ns prior to carrying out the PMF calculations and followed the same simulation procedure. For single ion PMF calculations, no other ions were within 14 Å of the target ion.[16] The ABF calculations of the PMF were carried out in different windows along the *z* direction (normal to the membrane) of the protein channel. The length of each ABF window was 5 Å except for regions near the receptor entrances, in which 10 Å was used.

The initial configuration for each ABF window was obtained from a 100ps equilibration simulation that had the target ion positioned within the window. For an ion to transport through the constricted TM pore (from *z*=-42 Å to *z*=-12 Å), no lateral restraints were applied on the target ion and production calculations of the PMF were continued for 5 ns. Outside the TM pore, the target ion was laterally restrained along the channel centerline (defined by the averaged mass center of pore lining residues in each ABF window) using harmonic restraints (with force constant of 0.5 kcal•mol^{-1}•Å^{-2}). The PMF calculation was performed for 2~3 ns in each window, or until the maximum free energy change was less than 0.3 Kcal/mol in 1 ns. Near the intracellular entrance (−57 Å < z < −42 Å), two calculations of Na^+ PMF were carried out each for 2 ns, during which the pore structure near E222 did not change much. Within each window the average force acting on the target ion was accumulated in 0.1 Å sized bins. The boundary force constant was set to be 10 Kcal/mol. The biasing force was applied only after the accumulation of 800 samples in individual bins.

V. MD calculations of the ion diffusion constants

In the bulk solution, diffusion constants for Na^+ and Cl^- were calculated using both mean squared displacement (MSD) method and random force autocorrelation function (FACF). Based on the MSD method,[17] the diffusion constant *D* along the z direction is calculated as:

$$D = \lim_{t\to\infty} \frac{\left\langle \Delta z(t)^2 \right\rangle}{2t} \qquad \text{(S1)}$$

where $\langle \Delta z(t)^2 \rangle$ is the mean squared displacement during a time period *t*. Same approach can be used to calculate the diffusion constant along x and y directions. The ion coordinate was collected every 10fs for a total of 4 ns MD simulations.

The FACF method is based on a generalized Langevin equation description of the ion motion. [18-20] It has previously been applied to calculate ion diffusivities in bulk liquids,[21,22] and in confined cavities or ion channels.[23,24] According to an approach used in Ref. 22 and 24 (the so-called second fluctuation dissipation theorem (SFDT) method in Ref 24), an ion is fixed at a specified position and the collected time series of the random force (described in more detail below) on that ion is used to compute the force-force autocorrelation function. Subsequently, the ion diffusivity (relevant for describing diffusive motion in the high friction regime, as assumed in our Brownian Dynamics simulations) in the z-direction is extracted via the formula: [23,24]

$$D = \frac{(k_B T)^2}{\int_0^\infty \langle R(0)R(t)\rangle dt} \qquad \text{(S2)}$$

where $R(0)$ and $R(t)$ are the z-direction random force at the initial time (t=0) and time t later than this, respectively. The same approach can be applied to estimate the ion diffusion constant in x and y directions. The random force was obtained by subtracting the time-averaged force (assumed equal to the equilibrium ensemble averaged force on the ion) from the instantaneous value of the systematic force.[23,24] In the simulations, a heavy atom (m=10^6 au) was assumed and a harmonic restraint of 10^4 Kcal/mol was applied to the ion. The systematic force on the ion was collected every 1fs for a total of 2~12 ns MD simulations depending on the ion positions. We calculated six ion diffusion constants along the channel centerline of System A at different positions (cf. Fig. S3), which broadly represented Na^+ ions in the middle of extracellular domain, inside the hydrophobic gate, and near the selectivity filer region.

Diffusion constants of Na^+ and Cl^- were measured experimentally as 1.33×10^{-5} cm^2/s and 2.02×10^{-5} cm^2/s in bulk water, respectively,[25] but they have not been determined inside an ion channel. Here we estimated the ion diffusion constants inside the GLIC channel using MD simulations. The MSD and FACF calculations resulted in the same diffusion constants of 1.9±0.2 $10^{-5}cm^2/s$ and 2.4±0.3 $10^{-5}cm^2/s$ for Na^+ and Cl^- in the bulk solutions, respectively. In the bulk solution, the calculated ion diffusion constants are the same along the x, y, z directions due to obvious spatial isotropy. Although the absolute values of these calculated diffusion constants are 20~40% greater than the experimental data, the calculated ratio of D_{Na}/D_{Cl} is in reasonable agreement with experimental results (0.66 vs 0.79).

The MSD method has been widely employed to calculate the diffusivities, but its application to narrow protein channels has found to be inappropriate.[24] The FACF method has been applied successfully to calculate the diffusion constants of a K^+ ion inside the narrow Gramicidin A channel.[24] Thus, inside the channel pore of GLIC we calculated diffusion constants of Na^+ and Cl^- using the FACF method only. The calculated ion diffusivity is highly correlated with the channel radii (cf. Fig. S3). Inside the EC domains, the ion diffusivity is roughly 0.5~1.0 (radii of 5~10 Å) times of its bulk value. Inside the TM domains, the ion diffusivity is 0.2~0.7 (2.5~6 Å) times of its bulk value. Furthermore, the calculated ion diffusion constants along the channel centerline are almost the same in the x, y, z directions.

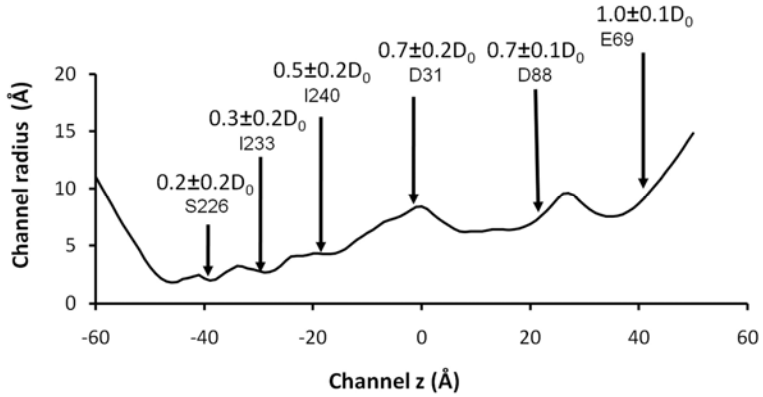

Figure S3: The calculated ion diffusivity for Na^+ ion inside the channel pore is highly correlated with the channel radius. The channel pore radius was averaged over 50 equilibrated GLIC structures. D_0 is the calculated bulk diffusivity for a Na^+ ion.

VI. Continuum calculation of electrostatic potential

The continuum electrostatics approach entails calculating the electrostatic potential energy ϕ in GLIC was obtained by solving Poisson's equation:

$$\nabla \cdot [\varepsilon \nabla \phi] = -4\pi\rho \quad , \qquad \text{(S3)}$$

where ε is the spatially dependent dielectric constant profile and ρ is the electric charge density due to partial charges of atoms in the protein channel. The probe radius for solvent was assumed to be 1.4 Å. Assignment of partial charges and dielectric constant profile for protein/membrane followed our previous procedure[26,27] and was based on the CHARMM27 force field. The effective dielectric constants for the TM domains (ε_{TMD}) and EC domains (ε_{ECD}) of the GLIC were assigned a value of 5 and 20 respectively, which fall within the range of previously adopted protein dielectric constants.[27-32] The membrane was assumed to be neutral with a dielectric constant $\varepsilon_M = 4$. The dielectric constant inside the aqueous pore (channel) was assumed to be the same as that in the bulk water, with $\varepsilon_w = 80$. Electrostatic energy calculations were carried out on a 155×155×205 lattice with 0.8 Å lattice spacing.

VII. Radial distribution function (RDF)

The dehydration information of a permeant Na^+ or Cl^- inside the channel was inferred from the radial distribution function (RDF) of the target ion and oxygen atoms (or hydrogen atoms for Cl^-) from the water molecules. RDF was calculated using VMD[3] and based on 500 trajectories from the last 1ns PMF calculations in System A. The number of atoms of the relevant species (n) surrounding the target ion with a cutoff of R was estimated using VMD. The first hydration shell for the target Na^+ or Cl^- inside the channel was estimated using a cutoff of 3.5 Å and 4.0 Å, respectively, where the first minima occur in g(r) after the first peaks.

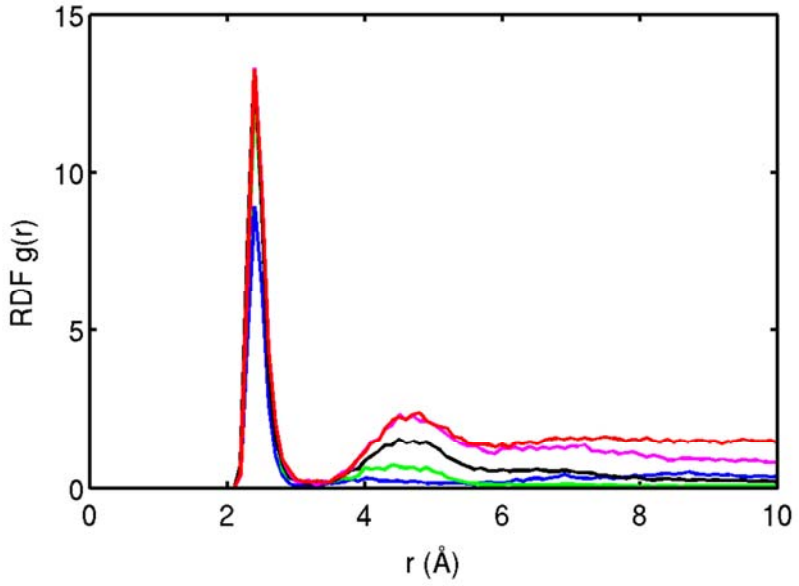

Figure S4: Radial distribution functions (RDF g(r)) of the target Na^+ ion and oxygen atoms from water near E222 (blue), T226 (green), I233 (black), E243 (pink) and bulk solution (red). E222 and T226 are near the intracellular entrance; I233 forms part of the hydrophobic gate [33]; and E243 is near the extracellular entrance. The target Na^+ ion was fully solvated with its first hydration shell through the entire channel pore except near E222, where partial dehydration was observed.

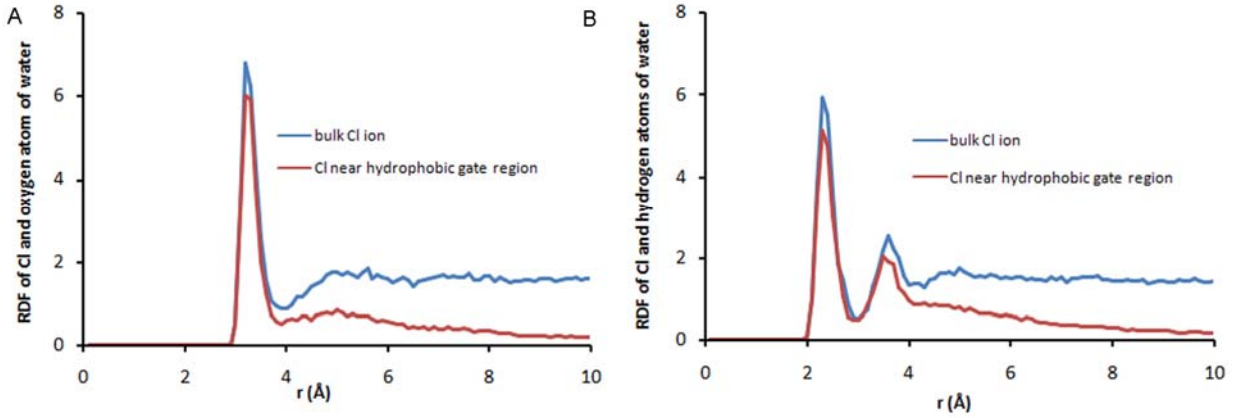

Figure S5: Partial dehydration was observed when a Cl^- ion transported through the hydrophobic gate region near I233. A) comparison of radial distribution function (RDF) of the target Cl^- ion and oxygen atoms from water in the bulk (blue) and hydrophobic gate region (red); and B) comparison of radial distribution function of the target Cl^- ion and hydrogen atoms from water in the bulk (blue) and hydrophobic gate (red). For a Cl^- ion, up to 15% reduction of its first hydration shell was observed.

VIII. Complete Author list for ref 28

(28) MacKerell, A. D., Bashford, D., Bellott, M., Dunbrack, R.L., Evanseck, J. D., Field, M. J., Fischer, S., Gao, J., Guo, H., Ha, S., Joseph-McCarthy, D., Kuchnir, L., Kuczera, K., Lau, F.T.K., Mattos, C., Michnick, S., Ngo, T., Nguyen, D. T., Prodhom, B., Reiher, W.E., Roux, B., Schlenkrich, M., Smith, J. C., Stote, R., Straub, J., Watanabe, M., Wiorkiewicz-Kuczera, J., Yin, D., Karplus, M. *J. Phys. Chem. B* **1998**, *102*, 3586–3616.

REFERENCES:

(1) Morris, G. M.; D.S., G.; Halliday, R. S.; Huey, R.; Hart, W. E.; Belew, R. K.; Olson, A. J. *J. Comput. Chem.* **1998**, *19*, 1639-1662.

(2) Chen, Q.; Cheng, M. H.; Xu, Y.; Tang, P. *Biophys. J.* **2010**, *99*, 1801-1809.

(3) Humphrey, W.; Dalke, A.; Schulten, K. *J. Mol. Graph.* **1996**, *14*, 33-38.

(4) Bocquet, N.; Nury, H.; Baaden, M.; Le Poupon, C.; Changeux, J. P.; Delarue, M.; Corringer, P. J. *Nature* **2009**, *457*, 111-114.

(5) Henderson, L. J. *Am. J. Physiol.* **1908**, *21*, 173-179.

(6) Hasselbalch, K. A. *Biochemische Zeitschrift* **1917**, *78*, 112-144.

(7) Chandler, D. E.; Hsin, J.; Harrison, C. B.; Gumbart, J.; Schulten, K. *Biophys. J.* **2008**, *95*, 2822-2836.

(8) Phillips, J. C.; Braun, R.; Wang, W.; Gumbart, J.; Tajkhorshid, E.; Villa, E.; Chipot, C.; Skeel, R. D.; Kale, L.; Schulten, K. *J. Comput. Chem.* **2005**, *26*, 1781-1802.

(9) MacKerell, A. D., Bashford, D., Bellott, M., Dunbrack, R.L., Evanseck, J. D., Field, M. J., Fischer, S., Gao, J., Guo, H., Ha, S., Joseph-McCarthy, D., Kuchnir, L., Kuczera, K., Lau, F.T.K., Mattos, C., Michnick, S., Ngo, T., Nguyen, D. T., Prodhom, B., Reiher, W.E., Roux, B., Schlenkrich, M., Smith, J. C., Stote, R., Straub, J., Watanabe, M., Wiorkiewicz-Kuczera, J., Yin, D., Karplus, M. *J. Phys. Chem. B* **1998**, *102*, 3586–3616.

(10) Hoover, W. *Phys. Rev. A.* **1985**, *31*, 1695.

(11) Nosé, S. *J. Chem. Phys.* **1984**, *81*, 511-519.
(12) Darden, T.; York, D.; Pedersen, L. *J Chem Phys* **1993**, *98*, 10089-10092.
(13) Chipot, C.; Hénin, J. *J. Chem. Phys.* **2005**, *123*, 244906.
(14) Darve, E.; Rodríguez-Gómez, D.; Pohorille., A. *J. Chem. Phys.* **2008**, *128*, 144120.
(15) Ivanov, I.; Cheng, X.; Sine, S. M.; McCammon, J. A. *J. Am. Chem. Soc.* **2007**, *129*, 8217-24.
(16) Allen, T. W.; Andersen, O. S.; Roux, B. *Biophys. J.* **2006**, *90*, 3447-3468.
(17) McQuarrie, D. A. *Statistical Mechanics*; Harper and Row: New York, 1976.
(18) Kubo, R. *Many-body Theory*; Syokabo and Benjamin: Tokyo, 1966.
(19) Zwanzig, R. W. *Annu. Rev. Phys. Chem.* **1965**, *16*, 67-102.
(20) Adelman, S. A. *Adv. Chem. Phys.* **1980**, *44*, 143-253.
(21) Straub, J. E.; Borkovec, M.; Berne, B. J. *J. Phys. Chem.* **1987**, *91*, 4995-4998.
(22) Koneshan, S.; Lynden-Bell, R. M.; Rasaiah, J. C. *J. Am. Chem. Soc.* **1998**, *120*, 12041-12050.
(23) Roux, B.; Karplus, M. *J. Phys. Chem.* **1991**, *95*, 4856-4868.
(24) Mamonov, A. B.; Kurnikova, M. G.; Coalson, R. D. *Biophys. Chem.* **2006**, 268-78.
(25) Hille, B. *Ion Channels of Excitable Membranes*; 3rd ed. ed.; Sinauer Assoc., Inc.: Sunderland, 2001.
(26) Kurnikova, M. G.; Coalson, R. D.; Graf, P.; Nitzan, A. *Biophys. J.* **1999**, *76*, 642-656.
(27) Haddadian, E. J.; Cheng, M. H.; Coalson, R. D.; Xu, Y.; Tang, P. *J. Phys. Chem. B* **2008**, *112*, 13981-90.
(28) Schutz, C. N.; Warshel, A. *Proteins* **2001**, *44*, 400-417.
(29) Cheng, M. H.; Mamonov, A. B.; Dukes, J. W.; Coalson, R. D. *J. Phys. Chem. B* **2007**, *111*, 5956-5965.
(30) Simonson, T.; C. L. Brooks, I. *J. Am. Chem. Soc.* **1996**, *118*, 8452–8458.
(31) Pitera, J. W.; Falta, M.; van Gunsteren, W. F. *Biophys. J.* **2001**, *80*, 2546–2555.
(32) Cheng, M. H.; Cascio, M.; Coalson, R. D. *Biophys. J.* **2005**, *89*, 1669-1680.
(33) Nury, H.; Poitevin, F.; Van Renterghem, C.; Changeux, J. P.; Corringer, P. J.; Delarue, M.; Baaden, M. *Proc Natl Acad Sci U S A* **2010**, *107*, 6275-80.